URSI-B EMTS 2025, Bologna, 23–27 June

Semi-Analytical Method for Electromagnetic Propagation in Biaxially Anisotropic Cylindrical Waveguides

Raul O. Ribeiro(1), Guilherme S. Rosa(1), Rafael A. Penchel(1), and Fernando L. Teixeira(2)
(1) School of Engineering, São Paulo State University, São João da Boa Vista, SP, Brazil
(2) Electroscience Laboratory, The Ohio State University, Columbus, OH, USA

Abstract

This paper introduces a semi-analytical method for decoupling and solving Maxwell's equations in biaxially anisotropic media expressed in cylindrical coordinates. The problem is reduced to a pair of coupled differential equations for the axial electric and magnetic fields, and conditions for their decoupling are examined. As a preliminary case study, we verify that the field solutions for a homogeneous anisotropic coaxial waveguide can be expressed as a linear combination of Bessel and Hankel functions of the first kind, generally with complex-valued, non-integer orders. This approach enables a reduction in the modal cutoff frequency, which is advantageous for minimizing waveguide dimensions in right-handed media and enables unconventional propagation characteristics in metamaterial devices.

1 Introduction

Anisotropic metamaterials have transformed the design of electromagnetic devices, offering properties that go far beyond those of conventional materials [1]. Anisotropic optical fibers allow for precise control of light polarization, which is crucial for maintaining signal integrity and advancing sensing capabilities [2, 3]. Metamaterials enable novel applications including advanced antennas and waveguides [4, 5]. In particular, waveguides filled with hyperbolic metamaterials have recently attracted significant attention. These materials are characterized by having one or two negative components in their dielectric permittivity tensor, while the remaining components are positive [6, 7, 8, 9]. Such anisotropic media can be fabricated using advanced techniques, including nanoporous dielectrics and thin-film layering [1, 10, 11, 12, 13].

The study and characterization of anisotropic materials pose significant challenges for numerical and semi-analytical methods. Fundamental issues have been identified in previous works [14, 15, 8] that rely on pre-assumed transverse magnetic (TM) and electric (TE) modal formulations for waveguides filled with biaxially anisotropic media. As demonstrated in [9], such structures, under general conditions, do not support decoupled wave propagation. In this context, the present work derives a necessary constitutive condition to achieve decoupled TM and TE modes. Additionally, as a case study, we developed a solution to model coaxial waveguides based on a linear combination of Bessel and Hankel functions. Depending on the anisotropy parameters, these functions may exhibit non-integer orders, which can be real or complex. This characteristic leads to unconventional propagation features, particularly advantageous for reducing waveguide dimensions.

2 Electromagnetic Field Modeling

Assuming and omitting the time-harmonic dependence $e^{-i\omega t}$, Maxwell's equations in a source-free, homogeneous and biaxially anisotropic media are

$$\nabla \times \mathbf{E} = i\omega\bar{\bar{\mu}} \cdot \mathbf{H}, \tag{1a}$$

$$\nabla \times \mathbf{H} = -i\omega\bar{\bar{\varepsilon}} \cdot \mathbf{E}, \tag{1b}$$

$$\nabla \cdot (\bar{\bar{\varepsilon}} \cdot \mathbf{E}) = 0, \tag{1c}$$

$$\nabla \cdot (\bar{\bar{\mu}} \cdot \mathbf{H}) = 0, \tag{1d}$$

where $\mathbf{E}$ and $\mathbf{H}$ are the electric and the magnetic fields, respectively. The media is characterized in cylindrical coordinates by the permeability

$$\bar{\bar{\mu}} = \text{diag}(\mu_\rho, \mu_\phi, \mu_z), \text{ with } \mu_\alpha = \mu_0\mu_{r\alpha} \tag{2}$$

and permittivity

$$\bar{\bar{\varepsilon}} = \text{diag}(\varepsilon_\rho, \varepsilon_\phi, \varepsilon_z), \text{ with } \varepsilon_\alpha = \varepsilon_0\varepsilon_{r\alpha} + i\sigma_\alpha/\omega \tag{3}$$

diagonal tensors, where σ_α is the anisotropic conductivity parameter. The tensors are expressed in terms of their components $\alpha \in \{\rho, \phi, z\}$ and the constitutive parameters are related to the usual vacuum constants ε_0 and μ_0.

Due to the symmetry of the problem in cylindrical geometries, field solutions assume a propagation factor of the form $\exp(ik_z + in\phi)$, where k_z is the corresponding axial wavenumber and n is an integer. We, by decomposing the problem into axial (along the z-direction) and transverse components, following the approach outlined in [16, pp. 164–165], and after several simplifications [14, 15, 17], we obtain a pair of coupled differential equations governing the axial electric and magnetic fields, as follows:

$$\mathscr{L}_e E_z = C_e \mathscr{L}_c H_z, \tag{4a}$$

$$\mathscr{L}_h H_z = C_h \mathscr{L}_c E_z, \tag{4b}$$

where $\mathscr{L}_e$ and $\mathscr{L}_h$ are Bessel differential operators given by

$$\mathscr{L}_g = \frac{1}{\rho}\frac{\partial}{\partial\rho}\rho\frac{\partial}{\partial\rho} + k_{g\rho}^2 - \frac{\nu_g^2}{\rho^2}, \quad \text{with} \quad g \in \{e,h\}, \tag{5}$$

the coupling operator is given by

$$\mathscr{L}_c = \frac{1}{\rho}\frac{\partial}{\partial\rho}, \tag{6}$$

and the remaining parameters are defined as

$$k_{e\rho}^2 = \frac{\varepsilon_z}{\varepsilon_\rho}(\omega^2\mu_\phi\varepsilon_\rho - k_z^2), \tag{7}$$

$$k_{h\rho}^2 = \frac{\mu_z}{\mu_\rho}(\omega^2\mu_\rho\varepsilon_\phi - k_z^2), \tag{8}$$

$$\nu_e^2 = n^2\frac{\varepsilon_\phi}{\varepsilon_\rho}\frac{\omega^2\mu_\phi\varepsilon_\rho - k_z^2}{\omega^2\mu_\rho\varepsilon_\phi - k_z^2}, \tag{9}$$

$$\nu_h^2 = n^2\frac{\mu_\phi}{\mu_\rho}\frac{\omega^2\mu_\rho\varepsilon_\phi - k_z^2}{\omega^2\mu_\phi\varepsilon_\rho - k_z^2}, \tag{10}$$

$$C_e = \frac{n k_z}{i\omega\varepsilon_\rho}\frac{\omega^2\mu_\rho\varepsilon_\phi - \omega^2\mu_\phi\varepsilon_\rho}{\omega^2\mu_\rho\varepsilon_\phi - k_z^2}, \tag{11}$$

$$C_h = \frac{n k_z}{i\omega\mu_\rho}\frac{\omega^2\mu_\rho\varepsilon_\phi - \omega^2\mu_\phi\varepsilon_\rho}{\omega^2\mu_\phi\varepsilon_\rho - k_z^2}. \tag{12}$$

The axial fields E_z and H_z are generally coupled in (4a) and (4b). However, the coupling vanishes under certain conditions of practical interest. Specifically, axial invariance ($k_z = 0$) or azimuthal invariance ($n = 0$) result in $C_{e,h} = 0$, causing the coupling in the differential equations (4a) and (4b) to disappear. Other decoupling scenarios arise when the condition

$$\mu_\rho\,\varepsilon_\phi = \mu_\phi\,\varepsilon_\rho \tag{13}$$

is satisfied. This special case includes isotropic and uniaxial anisotropic media, as will be clarified in the following discussion. For convenience, we proceed by defining the anisotropic parameters

$$\alpha_e^2 = \frac{\varepsilon_z}{\varepsilon_\rho}, \quad \alpha_h^2 = \frac{\mu_z}{\mu_\rho}, \quad \beta^2 = \frac{\varepsilon_\phi}{\varepsilon_\rho} = \frac{\mu_\phi}{\mu_\rho}. \tag{14}$$

By substituting the above into (4a) and (4b), the axial fields can be described by (decoupled) Bessel differential equations of order $\nu = \pm n\beta$, namely,

$$\left(\frac{1}{\rho}\frac{\partial}{\partial\rho}\rho\frac{\partial}{\partial\rho} + k_{e\rho}^2 - \frac{\nu^2}{\rho^2}\right)E_z = 0, \tag{15a}$$

$$\left(\frac{1}{\rho}\frac{\partial}{\partial\rho}\rho\frac{\partial}{\partial\rho} + k_{h\rho}^2 - \frac{\nu^2}{\rho^2}\right)H_z = 0. \tag{15b}$$

The appropriate selection of $\alpha_{e,h}$ and β enables the description of various practical scenarios, including:

- $\alpha_{e,h} = 1$ and $\beta = 1$: Isotropic media
- $\alpha_{e,h} = \beta$ and $\beta \neq 1$: Uniaxial (to ρ) anisotropic media
- $\alpha_{e,h} = 1$ and $\beta \neq 1$: Uniaxial (to ϕ) anisotropic media
- $\alpha_{e,h} \neq 1$ and $\beta = 1$: Uniaxial (to z) anisotropic media

3 Case Study of Coaxial Waveguides

Assuming the condition (13), we analyze a coaxial waveguide filled with biaxially anisotropic material and truncated by perfect electric conductors (PECs) at the boundaries $\rho = a$ and $\rho = b$. In view of (15a) and (15b), the solutions for the axial field components can be solved in a decoupled manner. Furthermore, we can verify that enforcing the boundary conditions allows for decoupled TM and TE modes in this scenario, with hybrid modes not being supported. This decoupling is not possible, for example, in layered media [18].

To analyze forward propagation along the z-axis ($z > 0$), an axial field can be expressed as [19]

$$G_z = \sum_{n=-\infty}^{\infty}\sum_{p=1}^{\infty} g_{z,np}(\rho)\, e^{in\phi + ik_{z,np}z}, \tag{16}$$

where $G = E$ and $g = e$ for the TM modes, and $G = H$ and $g = h$ for the TE modes. Here, n is an integer representing azimuthal dependence, while p denotes the radial dependence.

In view of (7), (8), and the decoupling condition (13), the axial wavenumber satisfy

$$k_{z,np}^2 = \beta^2\omega^2\mu_\rho\varepsilon_\rho - \frac{k_{g\rho,np}^2}{\alpha_g^2}, \quad \text{with} \quad g \in \{e,h\}. \tag{17}$$

The radial dependence function of the fields in (16) can be written with linear combinations of first-kind Bessel and Hankel functions [20, Ch. 10]

$$g_{z,np}(\rho) = A_g J_\nu(k_{g\rho,np}\rho) + B_g H_\nu^{(1)}(k_{g\rho,np}\rho), \tag{18}$$

where the order ν may be complex, A_g and B_g are constants determined by the boundary conditions, and the radial wavenumbers, $k_{g\rho,np}$, are determined by the zeros of the characteristic equation for the TM modes (19) and TE modes (20).

Given a fixed azimuthal index n, the characteristic equation for the solution (18) is expressed as

$$J_\nu(k_{e\rho,np}a)H_\nu^{(1)}(k_{e\rho,np}b) - J_\nu(k_{e\rho,np}b)H_\nu^{(1)}(k_{e\rho,np}a) = 0, \tag{19}$$

for the TM modes, and as

$$J'_\nu(k_{h\rho,np}a)H_\nu^{(1)\prime}(k_{h\rho,np}b) - J'_\nu(k_{h\rho,np}b)H_\nu^{(1)\prime}(k_{h\rho,np}a) = 0, \tag{20}$$

for the TE modes. The index p identifies each zero obtained when solving the characteristic equations (19) and (20) for a fixed n. In the above, the $'$ denotes differentiation with respect to the argument of the cylindrical functions. The recurrence relations, as defined in [20, Sec. 10.6], which are valid for complex-valued ν, can be applied:

$$J'_\nu(z) = \frac{\nu}{z}J_\nu(z) - J_{\nu+1}(z), \tag{21}$$

$$H_\nu^{(1)\prime}(z) = \frac{\nu}{z}H_\nu^{(1)}(z) - H_{\nu+1}^{(1)}(z). \tag{22}$$

4 Numerical Results

This section presents numerical results for illustrating the application of the formulation introduced in Section 3. The anisotropic coaxial waveguide is bounded internally and externally by PEC walls located at radii a and b, respectively, and it is filled with a material that ensures condition (13). The numerical computations were performed using Python, employing the *mpmath* library [21] to evaluate complex-order Bessel and Hankel functions. The zeros of the characteristic equations were computed using the Muller method, implemented via the *findroot* function provided by the *mpmath* library.

In the first scenario, we fix the azimuthal mode $n = 1$ and calculate the first radial waveguide constant, $p = 1$, for both TM and TE modes. We investigate positive and real-valued β^2, such as the order of the cylindrical functions become real-valued $\nu = \pm n\beta$. In this case, it is important to note that the two branches of solutions ($\pm$) yield fields that are linearly dependent, as demonstrated by the connection formulas in [20, 22, Sec. 10.4]. Figures 1 and 2 illustrate the radial wavenumbers as a function of the ratio a/b for various β^2 corresponding to TM_{11} and TE_{11} modes, respectively. In Figure 1, it can be observed that $k_{e\rho,11}$ exhibits minimal sensitivity to the anisotropy coefficient β^2. Conversely, in Figure 2, the mode associated with $k_{h\rho,11}$ demonstrates that selecting $\beta^2 < 1$ can effectively lower the cut-off frequencies. For both cases, $\beta^2 = 1$ corresponds to the isotropic scenario, where x_{11} and x'_{11} are the well-known first TM and TE modes (with $n = 1$ and $p = 1$) of a circular waveguide obtained in the limiting case $a/b \to 0$.

As a second scenario, we revisit the problem previously addressed in [8], which is characterized by the structural parameters $a = 100$ nm, $b = 250$ nm, and an axially hyperbolic anisotropic medium with $\varepsilon_{r\rho} = -1$, $\varepsilon_{r\phi} = 3.2883$, and $\varepsilon_{rz} = 3.2883$. The study presented in [8] contains a fundamental error, as the authors incorrectly assume solutions with decoupled TM and TE modes. However, this problem does not support decoupled waves, as demonstrated in [9]. Decoupled solutions can exist only if the constitutive parameters of the medium satisfy the condition specified in (13). To address this issue, we construct a solution where the condition (13) is satisfied, thereby ensuring the existence of decoupled TM and TE modes. Figure 3 shows the radial wavenumbers for TM and TE modes in the complex plane, considering $n \in \{0, 1, 2, 3\}$. In this scenario, the order ν is a purely imaginary number, necessitating the use of complex-order Bessel and Hankel functions in the characteristic equations (19) and (20). The obtained $k_{\rho e,h}$ values coincide with those of the isotropic case when $n = 0$, but significant differences arise for higher-order cases. Most notably, purely imaginary radial wavenumbers are observed for the first high-order modes (located along the vertical axis). This results in corresponding axial wavenumbers that are purely imaginary, characterizing evanescent modes. Conversely, modes with real-valued radial wavenumbers

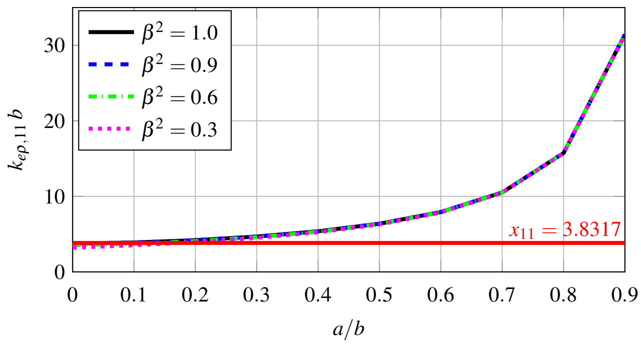

Figure 1. Normalized radial wavenumber $k_{e\rho,11}b$ for the TM_{11} mode as a function of the radius ratio a/b.

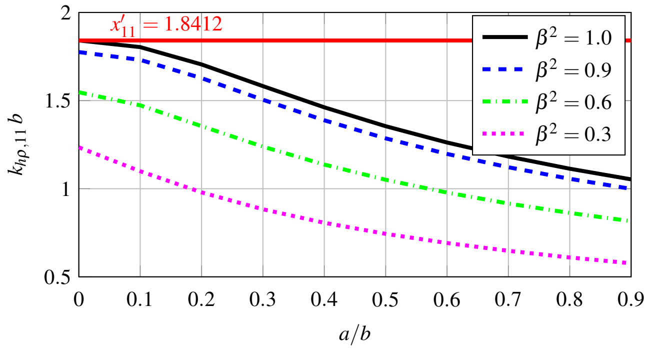

Figure 2. Normalized radial wavenumber $k_{h\rho,11}b$ for the TE_{11} mode as a function of the radius ratio a/b.

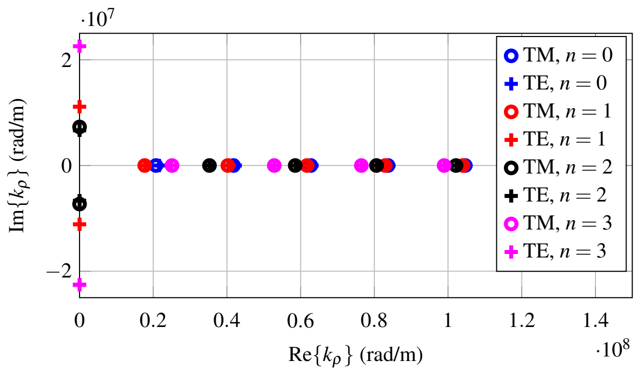

Figure 3. Radial wavenumbers for TM and TE modes in the complex plane considering $n \in \{0, 1, 2, 3\}$.

will yield real-valued k_z if $k_{g\rho}^2/\alpha_g^2 > \beta^2\omega^2|\mu_\rho\varepsilon_\rho|$. Interestingly, these high-order modes lack a low-frequency cutoff but exhibit instead a high-frequency cutoff.

5 Concluding Remarks and Look Ahead

This paper presented a semi-analytical approach for analyzing electromagnetic wave propagation in cylindrical biaxial anisotropic waveguides. We first derived a necessary condition for decoupled electric and magnetic fields and then constructed solutions using first-kind Bessel and Hankel functions to model TM and TE waves in coaxial waveguides. In the first example, we demonstrated the potential to lower modal waveguide cutoffs by setting $\beta^2 < 1$. The second example analyzed a coaxial waveguide filled with hyperbolic anisotropic media, revealing an unconventional cutoff behavior. Future work will extend this formulation to model multilayered waveguides, enabling precise characterization of metamaterial devices and anisotropic optical fibers.

6 Acknowledgment

This work was supported, in part, by the São Paulo State Research Foundation (FAPESP), Brazil, Process No. 2024/05690-0.

References

[1] D. R. Smith, J. B. Pendry, and M. C. K. Wiltshire, "Metamaterials and negative refractive index," *Science*, vol. 305, no. 5685, pp. 788–792, 2004.

[2] D. Gloge, "Weakly guiding fibers," *Applied Optics*, vol. 11, no. 11, pp. 2597–2600, 1972.

[3] K. Okamoto, *Fundamentals of Optical Waveguides*, 2nd ed. Elsevier, 2006.

[4] B. Donderici and F. L. Teixeira, "Metamaterial blueprints for reflectionless waveguide bends," *IEEE Microwave and Wireless Components Letters*, vol. 18, no. 4, pp. 233–235, 2008.

[5] T. J. Cui, D. R. Smith, and R. Liu, *Metamaterials*. Springer, 2010.

[6] R.-L. Chern, M.-C. Tsai, and Y.-Z. Yu, "Cylindrical plasmonic waveguides with cladding of hyperbolic metamaterials," *Journal of Lightwave Technology*, vol. 35, no. 10, pp. 1995–2002, 2017.

[7] A. Bhardwaj, K. V. Srivastava, and S. A. Ramakrishna, "Propagation of wave in a cylindrical waveguide filled with hyperbolic negative index medium," *Microwave and Optical Technology Letters*, vol. 62, no. 11, pp. 3385–3390, 2020.

[8] ——, "Enhanced coupling of light from subwavelength sources into a hyperbolic metamaterial fiber," *Journal of Lightwave Technology*, vol. 37, no. 13, pp. 3064–3072, 2019.

[9] A. Moradi and M. M. Bait-Suwailam, "Comment on: Enhanced coupling of light from subwavelength sources into a hyperbolic metamaterial fiber," *Journal of Lightwave Technology*, vol. 42, no. 15, pp. 5435–5436, 2024.

[10] B. Ghosh and A. B. Kakade, "Guided modes in a metamaterial-filled circular waveguide," *Electromagnetics*, vol. 32, no. 8, pp. 465–480, 2012.

[11] D. Pratap, S. A. Ramakrishna, J. G. Pollock, and A. K. Iyer, "Anisotropic metamaterial optical fibers," *Opt. Express*, vol. 23, no. 7, pp. 9074–9085, Apr. 2015.

[12] J. G. Pollock, A. K. Iyer, D. Pratap, and S. Anantha Ramakrishna, "A class of circular waveguiding structures containing cylindrically anisotropic metamaterials: Applications from radio frequency/microwave to optical frequencies," *J. Appl. Phys.*, vol. 119, no. 8, p. 083103, 2016.

[13] S. Tang, Y. Fang, L. Zhou, Z. Liu, and Y. Mei, "Anomalous scaling laws of hyperbolic metamaterials in a tubular geometry," *J. Opt. Soc. Am. B*, vol. 35, no. 2, pp. 391–395, Feb. 2018.

[14] J. R. Wait, "Electromagnetic response of an anisotropic conducting cylinder to an external source," *Radio Science*, vol. 13, no. 5, pp. 789–792, Sep. 1978.

[15] ——, "Correction to electromagnetic response of an anisotropic conducting cylinder to an external source," *Radio Science*, vol. 25, no. 06, pp. 1247–1247, Nov. 1990.

[16] J. Kong, *Electromagnetic Wave Theory*. New York, NY, USA: Wiley, 1986.

[17] J. R. Wait, "Electromagnetic surface impedance of an anisotropic cylinder," *IEE Proceedings A*, vol. 138, no. 3, pp. 184–186, May 1991.

[18] G. S. Rosa, "A robust method for solving the modal fields in radially unbounded cylindrical waveguides with two layers under extreme conductive conditions," *IEEE Trans. Antennas Propagat.*, vol. 70, no. 7, pp. 5841–5848, 2022.

[19] G. S. Rosa, J. R. Bergmann, and F. L. Teixeira, "A robust mode-matching algorithm for the analysis of triaxial well-logging tools in anisotropic geophysical formations," *IEEE Trans. Geosci. Remote Sens.*, vol. 55, no. 5, pp. 2534–2545, May 2017.

[20] "*NIST Digital Library of Mathematical Functions*," https://dlmf.nist.gov/, Release 1.2.3 of 2024-12-15, f. W. J. Olver, A. B. Olde Daalhuis, D. W. Lozier, B. I. Schneider, R. F. Boisvert, C. W. Clark, B. R. Miller, B. V. Saunders, H. S. Cohl, and M. A. McClain, eds. [Online]. Available: https://dlmf.nist.gov/

[21] F. Johansson *et al.*, "mpmath: A Python library for arbitrary-precision arithmetic," 2023, version 1.3. [Online]. Available: http://mpmath.org/

[22] G. S. Rosa, "An accurate and numerically stable formulation for computing the electromagnetic fields in uniform bend rectangular waveguides," *IEEE Trans. Microw. Theory Techn.*, vol. 71, no. 3, pp. 988–996, 2023.